BOREAL ENVIRONMENT RESEARCH 21: 230–241
ISSN 1239-6095 (print) ISSN 1797-2469 (online)

Helsinki 23 May 2016

On the accuracy of ion measurements using a Neutral cluster and Air Ion Spectrometer

Robert Wagner[1,*], Hanna E. Manninen[1], Alessandro Franchin[1], Katrianne Lehtipalo[1,2], Sander Mirme[3], Gerhard Steiner[4,5], Tuukka Petäjä[1] and Markku Kulmala[1,6]

[1)] *Department of Physics, P.O. Box 64, FI-00014 University of Helsinki, Finland (*corresponding author's e-mail: robert.wagner@helsinki.fi)*
[2)] *Paul Scherrer Institute, CH-5232 Villigen PSI, Switzerland*
[3)] *Institute of Physics, University of Tartu, Ulikooli 18, EE-50090 Tartu, Estonia*
[4)] *Faculty of Physics, University of Vienna, Boltzmanngasse 5, A-1090 Wien, Austria*
[5)] *Institute of Ion Physics and Applied Physics, Leopold-Franzens University, Innsbruck, Technikerstraße 25, A-6020 Innsbruck, Austria*
[6)] *Helsinki Institute of Physics, P.O. Box 64, FI-00014 University of Helsinki, Finland*

Received 1 Oct. 2015, final version received 22 Feb. 2016, accepted 18 Feb. 2016

Wagner R., Manninen H.E., Franchin A., Lehtipalo K., Mirme S., Steiner G., Petäjä T. & Kulmala M. 2016: On the accuracy of ion measurements using a Neutral cluster and Air Ion Spectrometer. *Boreal Env. Res.* 21: 230–241.

Here, we present a calibration of the Neutral cluster and Air Ion Spectrometer (NAIS, Airel Ltd.) for the size and concentration of ions in the mobility-diameter size-range 0.98–29.1 nm. Previous studies raised accuracy issues in size and concentration determination and highlighted the importance of used data inversion algorithm. Therefore, we investigated the performance of the NAIS by using five inversion methods. The presented results illustrate that the size information given by the NAIS is very accurate, regardless of the version of the data inversion. The number concentrations determined by the NAIS were 15%–30% too low especially at the lower end of the measurement size range (< 5 nm), whereas concentrations at diameters 19.6 nm and larger were overestimated by up to 8%. With the correction presented in this study, the uncertainty of the ion concentration measurement of the NAIS can be reduced to less than 10%, allowing the NAIS to be used in quantitative ion cluster studies and more accurate determination of formation and growth rates.

Introduction

Aerosol particles play a significant role in the global climate and e.g. in the water cycle. They affect the radiative forcing by directly absorbing and scattering sunlight. Acting as cloud condensation nuclei, aerosol particles also affect the lifetime and optical properties of clouds (Albrecht 1989). Many processes connected to secondary, freshly formed aerosol are not yet fully understood, e.g. nucleation and activation of clusters (Winkler *et al*. 2008, Jiang *et al*. 2011, Zhao *et al*. 2011, Kulmala *et al*. 2013). This is one reason why the quantitative effect of aerosol particles on the Earth's climate is still a rough estimate and the interest in nanometer-sized particles is

Editor in charge of this article: Hannele Korhonen

constantly growing. When investigating aerosol effects, one focus area is air ions, since they can play an important role in nucleation processes (Hirsikko *et al*. 2011, Kirkby *et al*. 2011). Some modeling studies underline the importance of ions (Yu and Turco 2000, 2008), while field measurements conducted with ion spectrometers suggest only minor contribution of ions to new particle formation within the continental boundary layer and in the lower atmosphere (Iida *et al*. 2006, Manninen *et al*. 2010, Mirme *et al*. 2010, Kulmala *et al*. 2013).

The Neutral cluster and Air Ion Spectrometer is one of the few instruments capable of detecting naturally charged ions and total (naturally charged and neutral) aerosol particles with a lower thresholds of 0.75 nm and 2 nm mobility diameters, respectively (Asmi *et al*. 2009, Manninen *et al*. 2011). This makes it suitable for observing new particle formation of both ions and total particles from an early stage (Kulmala *et al*. 2007, 2012, 2013). Moreover, the high time resolution up to one averaged number size distribution per second enables the observation of rapid processes.

The NAIS has been used for many years to determine ion and particle concentrations in various locations (Kulmala *et al*. 2007, 2013, Manninen *et al*. 2010, Rose *et al*. 2013, 2015) as well as in chamber studies (Kirkby *et al*. 2011, Franchin *et al*. 2015). Especially when determining the formation rate of ions or particles, or for the assessment of ion pair production rates and losses, the absolute number concentrations are of great importance.

Asmi *et al*. (2009) presented a laboratory comparison of ten ion spectrometers (5 NAISs and 5 AISs) and a Balanced Scanning Mobility Analyzer [BSMA, Tammet (2006)]. The results showed that the NAIS performed well overall, although some issues were identified. The ion mobilities were overestimated by about 40%, and at low ion concentrations the concentration values measured by the instrument were too high. The results of a follow-up intercomparison workshop (Gagne *et al*. 2011) demonstrated that the instruments, eleven ion spectrometers (6 NAISs and 5 AISs, including NAIS12 used in this study), still agreed well in general. However, a bias in the ion concentration measurement was observed again and background noise (electrometer signal without charges being collected) was identified as the main error source. Both studies highlighted the importance of the data inversion method, an algorithm to convert the measured electrometer currents as a function of mobility into ion number size distributions. The inversion routines (Mirme and Mirme 2013) used with the NAIS are based on model calculations simulating the trajectories of each ion entering the instrument; they take into account flow dynamics as well as diffusional losses.

The findings of Asmi *et al*. (2009) and Gagne *et al*. (2011) made clear that instrument modifications, and a redesign of the new generation of NAISs are needed. Some of the instruments used in the above mentioned studies are older versions which have not undergone the same technical improvements as the instrument in this study. Most important differences are a new flow scheme stabilizing the flows, and new data acquisition electronics with higher measurement frequency improving the signal to noise ratio.

We carried out calibration experiments with the NAIS in spring 2014 and 2015, focusing on the characterization of the mobility and concentration measurement of ions when deploying five different commonly applied versions of the data inversion algorithm. The need for the accuracy assessment emerged from ion cluster studies conducted at the CLOUD experiment [Cosmics Leaving Outdoor Droplets, Kirkby *et al*. (2011)] at CERN, where ion concentrations were used to determine ion production rates and losses. In this work, the particle mode was not considered. The aim of this study was to verify the concentration and mobility response of the instrument when using commonly applied versions of the inversion algorithm.

Methods

Instruments

Neutral cluster and Air Ion Spectrometer

The NAIS (Mirme and Mirme 2013) is an aerosol mobility spectrometer designed to determine the number size distribution of ions, as well as

total (naturally charged and neutral) particles in the mobility diameter range of 0.75–45 nm. It consists of two parallel differential mobility analyzers (DMAs) to simultaneously measure positive and negative ions. Each DMA is equipped with 21 electrometers, detecting charged particles of different mobilities. The instrument can periodically switch between an ion mode (measuring ions and naturally charged particles) and a particle mode (measuring naturally charged as well as neutral particles artificially charged with a corona charger). The instrument is described in more detail by Manninen *et al*. (2009) and Mirme and Mirme (2013). In this study, we used the instrument with serial the number NAIS12, which is identical to the instruments NAIS13–NAIS19. Using earlier versions of the instrument (< 12) may yield slightly different results due to earlier mentioned instrumental improvements; later versions (> 19) have an updated preconditioning unit with modified geometry to reduce its diffusional losses and to improve the uniformity of particle charging in particle measurement mode.

Differential mobility analyzers

The preparation of samples for the calibration measurements was done by using two different kinds of DMAs. For the selection of particles smaller than 5 nm mobility diameter, we used a Vienna type high resolution DMA (Herrmann *et al*. 2000), which was operated at 15 l min^{-1} sample flow rate and 797 l min^{-1} sheath flow rate. It has a resolution of $R = Z^*/\Delta Z_{1/2} = 17$, which is the ratio of the mobility at the peak of the transfer function Z^* to the full width at half maximum of the transfer function $\Delta Z_{1/2}$ (Flagan 1998). Thus the selected particles have a very high grade of monodispersity. The DMA was calibrated by using THAB (tetra-heptyl ammonium bromide) monomer mobility standard (Ude and de la Mora 2005). The calibration measurements for particles 14–30 nm mobility diameter were done by using a replica of a Vienna type Hauke DMA (Winklmayr *et al*. 1991). It was operated at 4 l min^{-1} sample flow rate and 20 l min^{-1} sheath flow rate. In this diameter range, it has an almost constant resolution of $R = 5$.

Reference counters

When measuring particles smaller than 5 nm, we used a TSI Electrometer 3068B as a reference for the concentration. It was operated at a sample flow rate of 2.5 l min^{-1}. According to the TSI manual, the current can be determined as accurate as ±1 fA (±150 cm^{-3}), while the uncertainty of the flow rate is ±5%.

For the calibration measurements in the size range larger than 14 nm, we used a Condensation Particle Counter (CPC) model TSI 3772, which has a cut-off diameter of 10 nm. Since the cut-off curve is not very steep, the concentrations were corrected for the counting efficiency provided by TSI. The manufacturer states an accuracy of the concentration measurement of ±10%.

Measurements and data analysis

Experimental setup and sample preparation

Different setups were used for particles smaller than 5 nm and 14–30 nm in diameter. Mobility diameters 5–14 nm were characterized by Gagne *et al*. (2011), ion concentrations were found to be well comparable to the reference instrument. Although obtained by using an earlier version of the instrument (NAIS5) and data inversion (amaisih06.sinp), those results are still valid. Technical improvements in later instruments and newer versions of the inversion algorithm mainly affected the detection of small ions (< 5 nm).

Small particles (< 5 nm) were generated with a tungsten wire aerosol generator (Kangasluoma *et al*. 2015), which was operated by using 15 l min^{-1} nitrogen 5.0 as a carrier gas. The sample mobility was selected with a Vienna type high resolution DMA (Fig. 1a). Larger particles were produced by atomizing an ammonium sulfate solution (carrier gas: 4 l min^{-1} dry filtered air), the size selection was done with a replica of a Vienna type Hauke DMA (Fig. 1b). Both DMAs were used with a ^{241}Am radioactive bipolar charger. Initially, we carried out measurements with both positive and negative ions, confirming that the response of the two analyzers in the NAIS is comparable (counting efficiencies matching within error limits). Therefore, in the

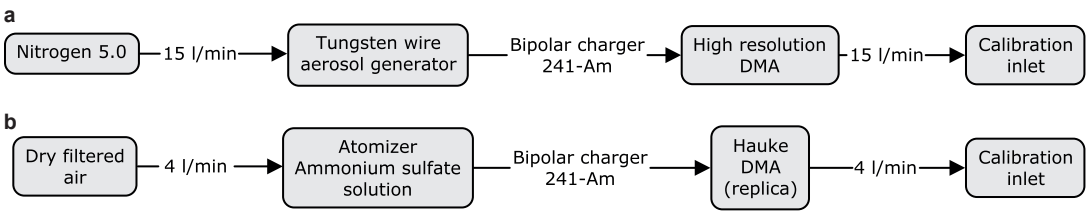

Fig. 1. (**a**) Experimental setups used for the calibration measurements. Aerosol particles smaller than 5 nm diameter were generated with a tungsten wire aerosol generator; the mobility was selected by a Vienna type high resolution DMA. (**b**) Particles of diameter 14–30 nm were generated atomizing an ammonium sulfate solution; size selection was done using a Hauke DMA.

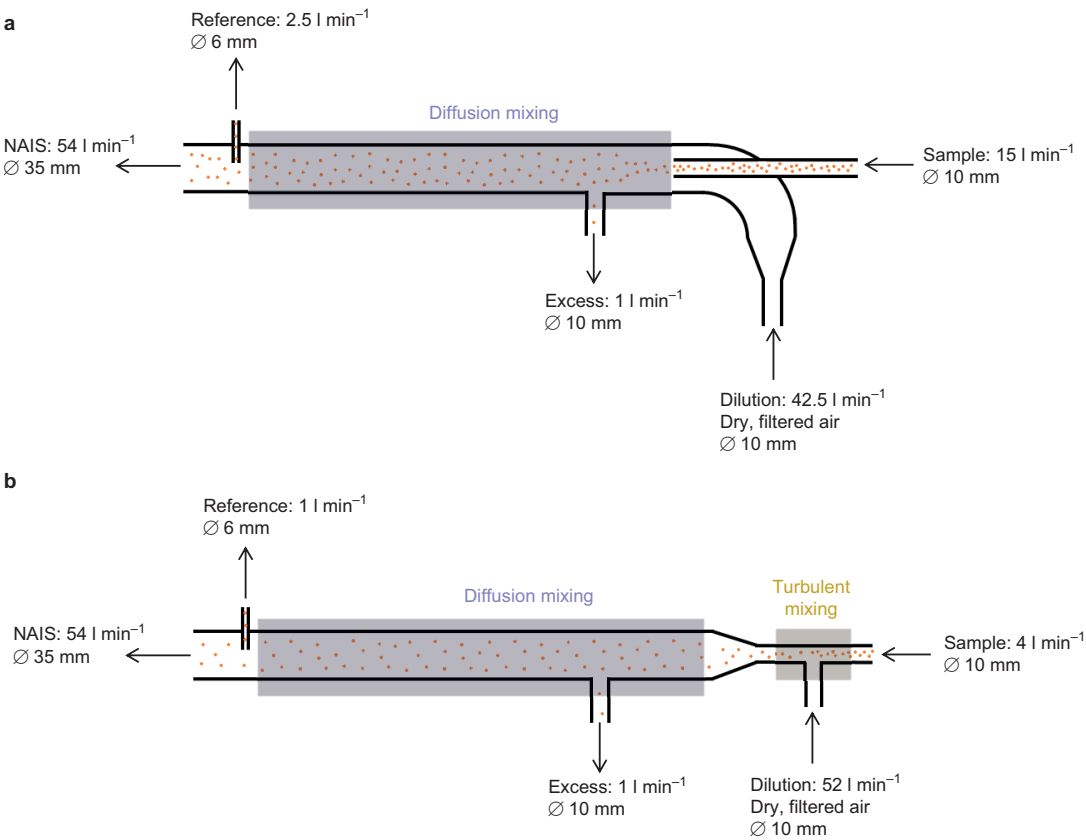

Fig. 2. Calibration inlets. The setup was slightly different for the size ranges (**a**) 0.98–4.42 nm and (**b**) 14.7–29.1 nm concerning the way how the dilution air flow was introduced and the length of the diffusion mixing section [(**a**) 50 cm and (**b**) 35 cm; Re = 2153].

subsequent experiments presented here, we used only negative ions.

Since the NAIS has a sample flow rate of 54 l min^{-1}, it was necessary to dilute the sample exiting the DMAs. Dilution of the sample is a very critical step and we designed the calibration inlets to ensure that the sample was mixed homogeneously before the sampling point (Fig. 2). Turbulent mixing was not used for small particles to avoid additional loss of sample aerosol and the signal getting too low. A small excess flow was necessary to balance the pressure. The reference counter was placed as close to the NAIS as possible. Additionally, we corrected the measured concentrations for diffusional losses in the sampling lines (Gormley and Kennedy

1948). The obtained ion concentrations after dilution were ranging from 100 to 10 000 cm^{-3}.

Data analysis

The sampling frequency of the NAIS12 is 12–13 Hz, spectra can be obtained with averaging times 1 s, 10 s or block (full cycle average). For the analysis we used spectra with a 10-second averaging time. This means that each spectrum included more than 120 measurements. The electrometer currents (raw data) measured by the NAIS were inverted by using five inversion algorithms (Mirme and Mirme 2013) to identify which one reproduces the reference measurements best. Since Airel Ltd. is updating the data inversion from time to time, to optimize the performance of the instrument, we investigated the currently most commonly used version (inv3) as well as earlier and later versions (Table 1). The main differences in inversion algorithms concern the estimation of the diffusional losses, a fault increasing the average ion concentration at low signals ('positive bias fault'; affecting background), and the application of a negative concentration correction algorithm.

The accuracy in sizing was estimated by fitting a Gaussian curve to the average number size distribution measured with the NAIS (arithmetic mean of 64–191 spectra). The position of the maximum (mode diameter) was then compared with the diameter selected with the DMA (Fig. 3). The uncertainty of the detected diameter was estimated by using the full width at half maximum of the Gaussian curve. To investigate the error in the concentration measurements, the values obtained with the NAIS (integrated concentration over the range of the peak) were plotted against the reference data and a linear fit ($y = ax + b$) was applied. The slope of the fit indicated the counting efficiency of the NAIS (Fig. 4). The uncertainties of the counting efficiencies were approximated by applying a linear fit to the lower and the upper limits of the confidence intervals of the reference measurements (shaded areas in Fig. 4). The concentration correction coefficients were obtained by fitting power law functions [$f(d_p) = a(d_p)^b$] to the determined counting efficiencies of the NAIS. The uncertainties of the fit parameters are the 95%CIs of the fit.

The particle mobilities were converted to diameters according to the Millikan-Fuchs relation, $Z_p = neB$, as described by Mäkelä *et al.* (1996), where Z_p is the electrical mobility, n the number of elementary charges, e the elementary charge and B the mechanical mobility. We assumed all particles to be singly charged, the experiments were designed to keep the amount of multiply charged particles negligible.

Results

We evaluated the data from 64–191 NAIS ion spectra (10 s averaging time) for each investigated diameter. Uncertainties of the selected mobility diameters were estimated accounting

Table 1. Data inversion algorithms (Mirme and Mirme 2013) investigated in this study, their abbreviations and main differences. The diffusion loss parameter is an empirical parameter that is chosen for the diffusion loss function based on the instrument calibration. Internally the parameter determines the equivalent path length for particles in the diffusion loss model. The positive bias fault is an error in the inversion algorithm creating a statistical bias increasing concentrations where an electrometer signal was negative. The negative concentration correction algorithm is a method used in the data inversion procedure that tries to remove negative concentrations from the inversion result distributions and improve the quality of the measurement results while avoiding the increase of average concentrations.

Code	Inversion algorithm	Diffusion loss parameter	Positive bias fault	Negative concentration correction algorithm
inv1	amnais012-20140228	0.035	no	yes
inv2	amnais012-20140303	0.035	no	no
inv3	amnais13	0.050	yes	yes
inv4	amnais13-20140228	0.050	no	yes
inv5	v14-lrnd	0.035	no	yes

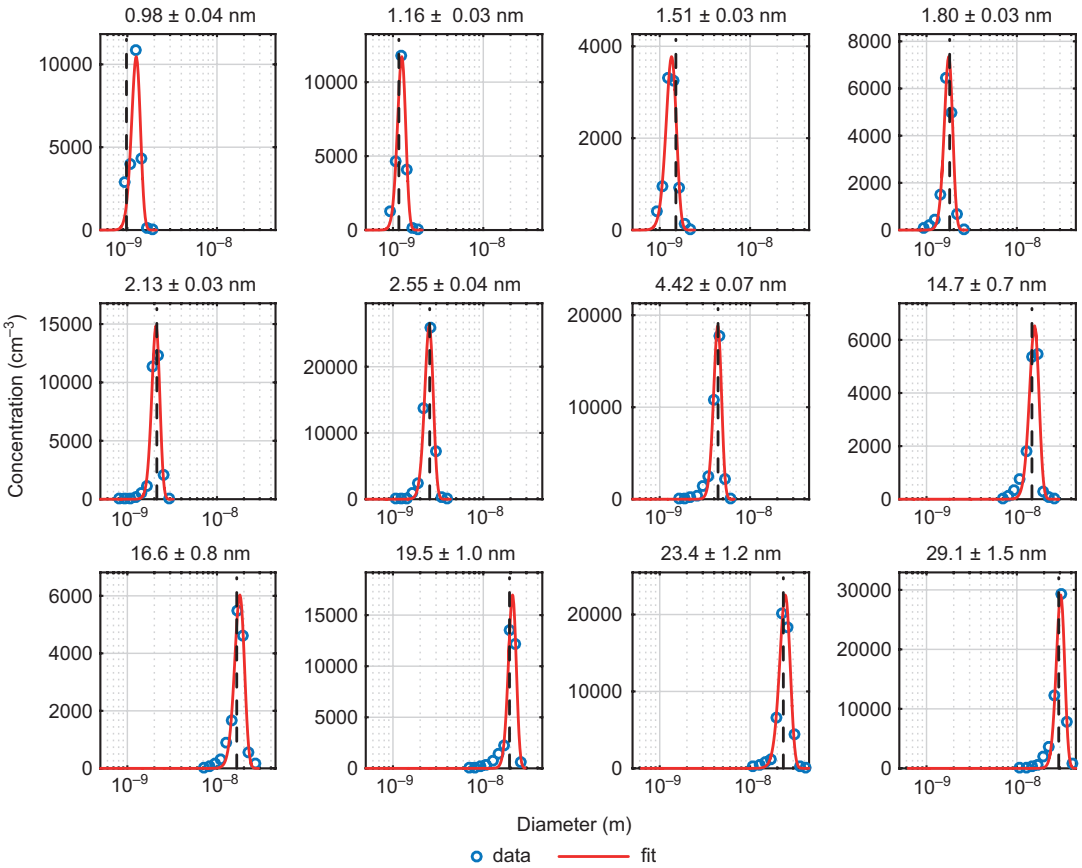

Fig. 3. Size calibration for each sample diameter. The circles mark the number size distribution measured with the NAIS (data inversion method inv5), the red line is a Gaussian fit and the black dashed line marks the diameter selected by the DMA (values displayed above each plot; < 5 nm: high resolution DMA, > 5 nm: Hauke DMA).

for the resolution of the DMAs as well as the possible fluctuations of the high voltage supply. The mode diameter determined from number size distributions measured by the NAIS is very accurate. Especially in the size range 1.80–4.42 nm the mode diameter matches the diameter selected by the DMA within 1% (Fig. 5a). For example, for the latest version of the inversion inv5 the ratio of detected to selected diameter is on average 0.99 ± 0.03. However, at the lower end of the measurement size range (1.5 nm and smaller) the NAIS was not able to distinguish between the mobilities anymore; the detected mode diameter hardly changed between the sample diameters 0.98 nm, 1.16 nm and 1.51 nm. The slope of the linear fit for sample diameters 1.80–4.42 nm equals unity within error limits, which demonstrates the high accuracy of the determined mode diameters. At diameters larger than 14 nm, the NAIS slightly overestimated the particle diameter, on average by 6% (Fig. 5b). Furthermore, our results indicate that the choice of the data inversion algorithm has a negligible effect on the size information obtained by the NAIS (Fig. 5). The detected diameters showed little variation between different inversion methods.

When verifying the concentration measurements, we found a size dependence in the counting efficiency of the instrument (*see* Fig. 6). Three out of five versions led to very similar results underestimating concentrations of small ions by up to 30% at diameters 0.98–4.42 nm mobility diameter and overestimating ion concentrations by up to 8% in the range 14.7–29.1 nm. However, inv3 and inv4 produced very different values at diameters < 3 nm than the other three versions, overestimating the concentrations of ions smaller than 1.51 nm mobility diameter

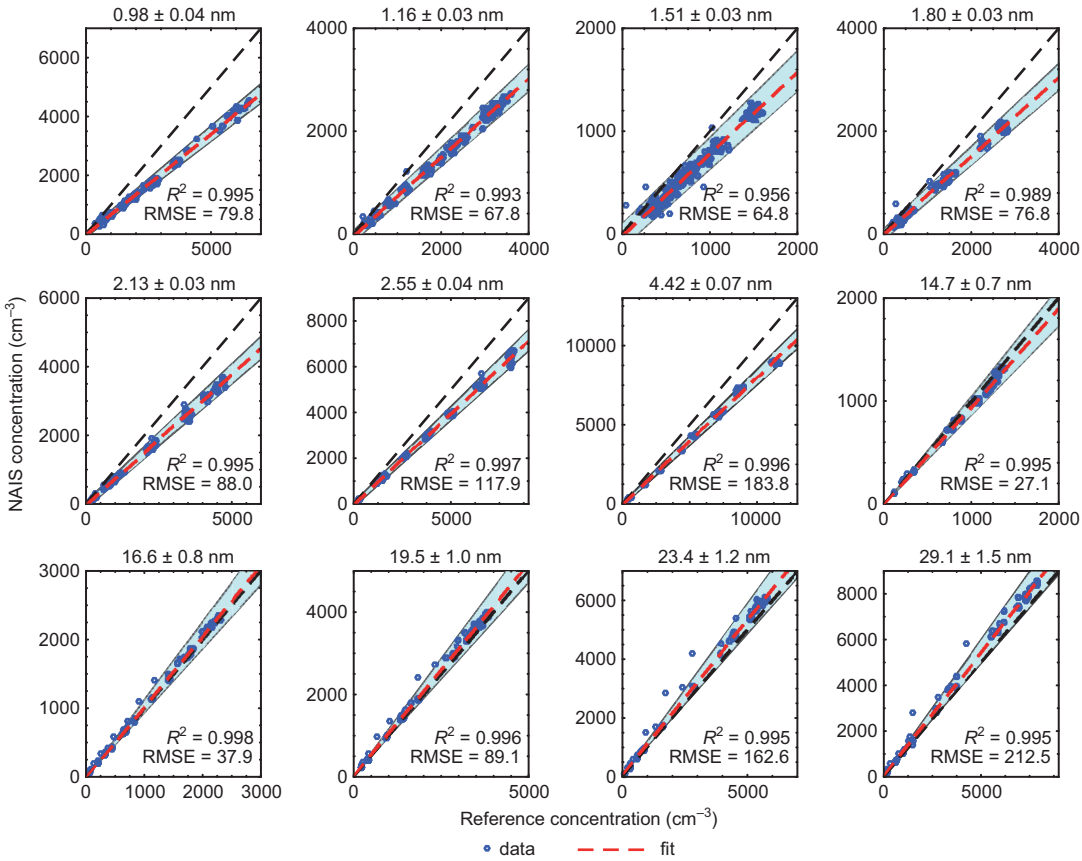

Fig. 4. Concentration calibration for each sample diameter (values above each plot). Ion concentrations measured with the NAIS (data inversion method inv5) as a function of ion concentrations determined by a reference counter (0.98–4.42 nm: TSI Electrometer 3068B; 14.7–29.1 nm: TSI CPC 3772) for all investigated diameters. The shaded areas are the 95%CIs of the fit, taking into account the uncertainty of the reference counter. Ideally, the fit (red dashed line, $y = ax + b$) would match the one-to-one line (black dashed line).

by up to 30% (Fig. 6). Since the other inversion methods showed consistent behavior, we were able to apply a power law fit (Table 2) which represented the data well ($R^2 \geq 0.94$). We used these functions to derive counting efficiencies (transmission) for each diameter in the NAIS ion spectrum (Table 3). As a summary, the NAIS (using the consistent inversion algorithms inv1, inv2 and inv5) underestimated ion concentrations by up to 30% at the lower end of the measurement size range; at diameters larger than 16 nm the concentrations given by the instrument were up to 8% higher than those shown by the reference instruments. The concentration response of the NAIS was linear at all sizes and concentrations (Fig. 4).

By using the power law fit functions (Table 2), we derived correction factors for the concentration in each size bin in the measurement size range (Table 3). These values correspond to the transmission of the instrument. Dividing the measured concentrations by the transmission values yields the actual concentration. With those terms applied to the concentrations measured by the NAIS, the concentration values agreed with the reference within 10% (inv1: ±5.9%, inv2: ±6.7%, inv5: ±7.1%; *see* Fig. 7).

Discussion

By careful laboratory calibrations, we demonstrated that the size information given by the NAIS was very accurate at sizes larger than

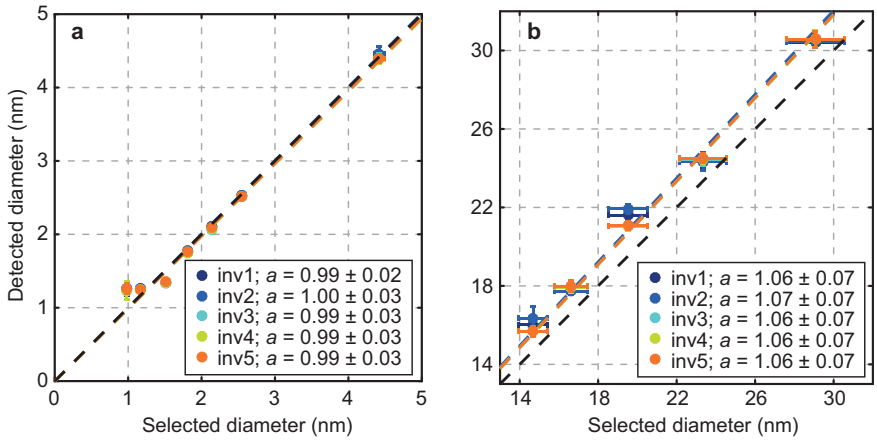

Fig. 5. Accuracy of mobility diameters measured with the NAIS. Detected diameter (mode diameter from a Gaussian fit) as a function of selected diameter (< 5 nm: high resolution DMA, > 5 nm: Hauke DMA). The slopes of the linear fits ($y = ax$) are indicated in the legend. The black dashed line represents the one-to-one line. Since the NAIS does not resolve sizes at 1.5 nm and below, the fit in **a** does not include those three data points.

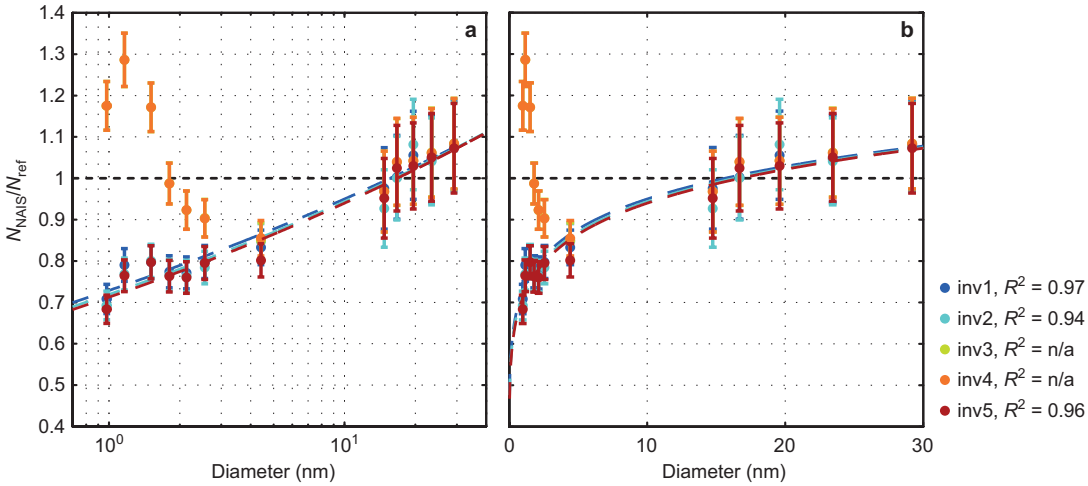

Fig. 6. NAIS counting efficiency as a function of mobility diameter comparing five data inversion algorithms; for better visualization of the changes, the results are shown on (**a**) logarithmic scale and (**b**) linear scale. Each point in the figure represents the results of at least 64 measurements, evaluating the performance at different ion concentrations. The error bars are 95%CIs and correspond to the shaded areas around the fit in Fig. 4 (*see* section 'Data analysis' for more details). The power law fit (Table 2) matches the data points well (coefficients of determinations R^2 are given in the legend in **b**). Data obtained using inv3 and inv4 could not be approximated by the fit (green and orange; the results are very similar, green dots are covered by the orange dots).

Table 2. Coefficients to derive the transmission values from the fit function $f(d_p) = a(d_p)^b$ with $[d_p]$ = [nm].

Inversion method	*a*	*b*
inv1	0.729 ± 0.026	0.115 ± 0.015
inv2	0.719 ± 0.035	0.118 ± 0.021
inv5	0.713 ± 0.030	0.120 ± 0.018

1.5 nm. At diameters 1.80–4.42 nm the mode diameter matched the selected mobility diameters within 1% (e.g. inv5: the ratio $d_{p,NAIS}$ to $d_{p,REF}$ was on average a = 0.99 ± 0.03; *see* Fig. 5a). At sample diameters larger than 14 nm the mode diameter was overestimated by on average 6% (inv1, inv3–inv5: a = 1.06 ± 0.07; *see* Fig. 5b). However, the smallest sample diameters (≤ 1.5 nm) could not be distinguished from

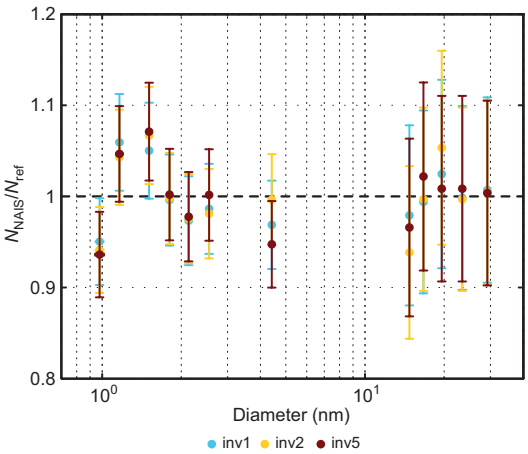

Fig. 7. NAIS counting efficiency as a function of particle diameter after applying the correction terms (Table 3) for inversion methods inv1, inv2 and inv5.

each other. Modifying the preconditioning unit or reducing the size range of the instrument may improve the resolution at the smallest diameters. All analyzed inversion methods led to similar results and the concentration response of the NAIS was linear at all sizes, also towards low concentrations (Fig. 4). Therefore, with the instrument and inverters used in this study, our results agree with those of Gagne *et al*. (2011). Contrary to Asmi *et al*. (2009), we did not find the overestimation of ion concentrations by 40% at low concentrations any longer. It is likely that the positive bias fault was present in the inversion method used by Asmi *et al*. (2009). This is an error in the inversion algorithm which created a statistical bias increasing concentrations where an electrometer signal was negative. Negative signals occur frequently due to measurement noise when the particle concentrations are very

Table 3. Transmission values for ion concentrations determined using inversion methods inv1, inv2 or inv5. The uncertainties represent the 95%CIs.

Channel no.	$d_{p,mean}$ (nm)	inv1		inv2		inv5	
		factor	uncertainty	factor	uncertainty	factor	uncertainty
1	0.81	0.711	0.023	0.702	0.031	0.695	0.027
2	0.94	0.724	0.025	0.714	0.034	0.707	0.029
3	1.08	0.735	0.027	0.726	0.036	0.719	0.032
4	1.25	0.748	0.029	0.738	0.039	0.732	0.034
5	1.44	0.760	0.031	0.751	0.042	0.744	0.037
6	1.66	0.773	0.034	0.763	0.045	0.757	0.039
7	1.92	0.786	0.036	0.777	0.048	0.771	0.042
8	2.21	0.798	0.038	0.790	0.051	0.784	0.045
9	2.56	0.812	0.041	0.804	0.054	0.798	0.048
10	2.96	0.826	0.043	0.817	0.058	0.812	0.051
11	3.41	0.839	0.046	0.831	0.061	0.826	0.054
12	3.94	0.853	0.049	0.845	0.065	0.840	0.057
13	4.56	0.868	0.051	0.860	0.069	0.855	0.060
14	5.27	0.882	0.054	0.875	0.072	0.870	0.064
15	6.09	0.897	0.057	0.890	0.076	0.885	0.067
16	7.04	0.912	0.060	0.905	0.080	0.901	0.071
17	8.15	0.928	0.063	0.921	0.085	0.917	0.074
18	9.42	0.943	0.066	0.937	0.089	0.933	0.078
19	10.9	0.959	0.070	0.953	0.093	0.950	0.082
20	12.6	0.976	0.073	0.970	0.098	0.966	0.086
21	14.6	0.992	0.077	0.987	0.103	0.984	0.090
22	16.9	1.009	0.080	1.004	0.108	1.001	0.095
23	19.6	1.026	0.084	1.022	0.113	1.019	0.099
24	22.8	1.044	0.088	1.040	0.118	1.038	0.104
25	26.4	1.062	0.092	1.058	0.123	1.056	0.109
26	30.7	1.081	0.096	1.077	0.129	1.076	0.114
27	35.7	1.100	0.100	1.097	0.135	1.095	0.119
28	41.6	1.119	0.104	1.116	0.141	1.116	0.124

low. This error would typically affect the background concentrations.

On the other hand, the concentration values provided by the NAIS depended strongly on the algorithm used for data inversion. The results of all inversion methods were comparable for diameters larger than 4 nm, whereas inverters inv3 and inv4, which are most commonly used, led to very different values at smaller diameters. For the data obtained by using those inverters, we recommend to perform a new inversion (using inv1, inv2 or inv5) and correct the data by using the transmission terms provided in this study (Table 3). Data obtained by using one of the consistent inverters (inv1, inv2, inv5) do not need to be re-inverted, however, they should be corrected with the corresponding factors (Table 3). Applying the proposed procedure, the ion concentrations are accurate within ±10% (inv1: ±5.9%, inv2: ±6.7%, inv5: ±7.1%, Fig. 7).

Our results can be directly applied to the instruments NAIS12–NAIS19 (identically constructed), however, using earlier or later versions may yield slightly different results. The newest versions of the NAIS (> 19) have at present a modified preconditioning unit (adjusted geometry) to decrease its diffusional losses, and to improve the uniformity of particle charging in particle measurement mode.

Atmospheric new particle formation is a global phenomenon (Kulmala *et al*. 2004) and reliable direct measurements are needed to further understand it. To find out proper formation and growth rates (Kulmala *et al*. 2012, 2013), accurate information on size and concentration is crucial. This way the uncertainties in atmospheric model parameterizations can be decreased. The present results enable using the NAIS for reliable ion cluster measurements and determining formation and growth rates more precisely.

Acknowledgements: This research was funded by the EC Seventh Framework Programme (Marie Curie Initial Training Network MC-ITN "CLOUD-TRAIN" no. 316662, ERC-Advanced "ATMNUCLE"' grant no. 227463), the European Union's Horizon 2020 research and innovation programme under the Marie Sklodowska-Curie grant agreement no. 656994, the Austrian Science Fund FWF (grant no. P27295-N20), and the Academy of Finland Centre of Excellence (grant no. 272041).

References

Albrecht B.A. 1989. Aerosols, cloud microphysics, and fractional cloudiness. *Science* 245: 1227–1230.

Asmi E., Sipilä M., Manninen H.E., Vanhanen J., Lehtipalo K., Gagne S., Neitola K., Mirme A., Mirme S., Tamm E., Uin J., Komsaare K., Attoui M. & Kulmala M. 2009. Results of the first air ion spectrometer calibration and intercomparison workshop. *Atmospheric Chemistry and Physics* 9: 141–154.

Flagan R.C. 1998. History of electrical aerosol measurements. *Aerosol Science and Technology* 28: 301–380.

Franchin A., Ehrhart S., Leppä J., Nieminen T., Gagné S., Schobesberger S., Wimmer D., Duplissy J., Riccobono F., Dunne E.M., Rondo L., Downard A., Bianchi F., Kupc A., Tsagkogeorgas G., Lehtipalo K., Manninen H.E., Almeida J., Amorim A., Wagner P.E., Hansel A., Kirkby J., Kürten A., Donahue N.M., Makhmutov V., Mathot S., Metzger A., Petäjä T., Schnitzhofer R., Sipilä M., Stozhkov Y., Tomé A., Kerminen V.-M., Carslaw K., Curtius J., Baltensperger U. & Kulmala M. 2015. Experimental investigation of ion–ion recombination under atmospheric conditions. *Atmospheric Chemistry and Physics* 15: 7203–7216.

Gagne S., Lehtipalo K., Manninen H.E., Nieminen T., Schobesberger S., Franchin A., Yli-Juuti T., Boulon J., Sonntag A., Mirme S., Mirme A., Horrak U., Petäjä T., Asmi E. & Kulmala M. 2011. Intercomparison of air ion spectrometers: an evaluation of results in varying conditions. *Atmospheric Measurement Techniques* 4: 805–822.

Gormley P.G. & Kennedy M. 1948. Diffusion from a stream flowing through a cylindrical tube. *Proceedings of the Royal Irish Academy A* 52: 163–169.

Herrmann W., Eichler T., Bernardo N. & de la Mora J.F. 2000. *Turbulent transition arises at Reynolds number 35,000 in a short Vienna type DMA with a large laminarization inlet*. Abstract, Annual Conference of the AAAR, St. Louis, USA.

Hirsikko A., Nieminen T., Gagne S., Lehtipalo K., Manninen H.E., Ehn M., Horrak U., Kerminen V.-M., Laakso L., McMurry P.H., Mirme A., Mirme S., Petäjä T., Tammet H., Vakkari V., Vana M. & Kulmala M. 2011. Atmospheric ions and nucleation: a review of observations. *Atmospheric Chemistry and Physics* 11: 767–798.

Iida K., Stolzenburg M., McMurry P., Dunn M.J., Smith J.N., Eisele F. & Keady P. 2006. Contribution of ion-induced nucleation to new particle formation: Methodology and its application to atmospheric observations in Boulder, Colorado. *Journal of Geophysical Research-Atmospheres* 111: D23201, doi: 10.1029/2006JD007167.

Jiang J.K., Zhao J., Chen M.D., Eisele F.L., Scheckman J., Williams B.J., Kuang C.A. & McMurry P.H. 2011. First measurements of neutral atmospheric cluster and 1–2 nm particle number size distributions during nucleation events. *Aerosol Science and Technology* 45: ii–v.

Kangasluoma J., Attoui M., Junninen H., Lehtipalo K., Samodurov A., Korhonen F., Sarnela N., Schmidt-Ott A., Worsnop D., Kulmala M. & Petäjä T. 2015. Sizing of

neutral sub 3 nm tungsten oxide clusters using Airmodus Particle Size Magnifier. *Journal of Aerosol Science* 87: 53–62.

Kirkby J., Curtius J., Almeida J., Dunne E., Duplissy J., Ehrhart S., Franchin A., Gagne S., Ickes L., Kürten A., Kupc A., Metzger A., Riccobono F., Rondo L., Schobesberger S., Tsagkogeorgas G., Wimmer D., Amorim A., Bianchi F., Breitenlechner M., David A., Dommen J., Downard A., Ehn M., Flagan R.C., Haider S., Hansel A., Hauser D., Jud W., Junninen H., Kreissl F., Kvashin A., Laaksonen A., Lehtipalo K., Lima J., Lovejoy E.R., Makhmutov V., Mathot S., Mikkilä J., Minginette P., Mogo S., Nieminen T., Onnela A., Pereira P., Petäjä T., Schnitzhofer R., Seinfeld J.H., Sipilä M., Stozhkov Y., Stratmann F., Tome A., Vanhanen J., Viisanen Y., Vrtala A., Wagner P.E., Walther H., Weingartner E., Wex H., Winkler P.M., Carslaw K.S., Worsnop D.R., Baltensperger U. & Kulmala M. 2011. Role of sulphuric acid, ammonia and galactic cosmic rays in atmospheric aerosol nucleation. *Nature* 476: 429–433.

Kulmala M., Vehkamäki H., Petäjä T., Dal Maso M., Lauri A., Kerminen V.-M., Birmili W. & McMurry P.H. 2004. Formation and growth rates of ultrafine atmospheric particles: a review of observations. *Journal of Aerosol Science* 35: 143–176.

Kulmala M., Petäjä T., Nieminen T., Sipilä M., Manninen H.E., Lehtipalo K., Dal Maso M., Aalto P.P., Junninen H., Paasonen P., Riipinen I., Lehtinen K.E.J., Laaksonen A. & Kerminen V.-M. 2012. Measurement of the nucleation of atmospheric aerosol particles. *Nature Protocols* 7: 1651–1667.

Kulmala M., Riipinen I., Sipilä M., Manninen H.E., Petäjä T., Junninen H., Dal Maso M., Mordas G., Mirme A., Vana M., Hirsikko A., Laakso L., Harrison R.M., Hanson I., Leung C., Lehtinen K.E.J. & Kerminen V.-M. 2007. Toward direct measurement of atmospheric nucleation. *Science* 318: 89–92.

Kulmala M., Kontkanen J., Junninen H., Lehtipalo K., Manninen H.E., Nieminen T., Petäjä T., Sipilä M., Schobesberger S., Rantala P., Franchin A., Jokinen T., Järvinen E., Äijälä M., Kangasluoma J., Hakala J., Aalto P.P., Paasonen P., Mikkilä J., Vanhanen J., Aalto J., Hakola H., Makkonen U., Ruuskanen T., Mauldin R.L., Duplissy J., Vehkamäki H., Bäck J., Kortelainen A., Riipinen I., Kurten T., Johnston M.V., Smith J.N., Ehn M., Mentel T.F., Lehtinen K.E.J., Laaksonen A., Kerminen V.-M. & Worsnop D.R. 2013. Direct observations of atmospheric aerosol nucleation. *Science* 339: 943–946.

Mäkelä J.M., Riihela M., Ukkonen A., Jokinen V. & Keskinen J. 1996. Comparison of mobility equivalent diameter with Kelvin-Thomson diameter using ion mobility data. *Journal of Chemical Physics* 105: 1562–1571.

Manninen H.E., Petäjä T., Asmi E., Riipinen I., Nieminen T., Mikkilä J., Horrak U., Mirme A., Mirme S., Laakso L., Kerminen V.-M. & Kulmala M. 2009. Long-term field measurements of charged and neutral clusters using Neutral cluster and Air Ion Spectrometer (NAIS). *Boreal Environment Research* 14: 591–605.

Manninen H.E., Franchin A., Schobesberger S., Hirsikko A., Hakala J., Skromulis A., Kangasluoma J., Ehn M., Junninen H., Mirme A., Mirme S., Sipilä M., Petäjä T., Worsnop D.R. & Kulmala M. 2011. Characterisation of corona-generated ions used in a Neutral cluster and Air Ion Spectrometer (NAIS). *Atmospheric Measurement Techniques* 4: 2767–2776.

Manninen H.E., Nieminen T., Asmi E., Gagné S., Häkkinen S., Lehtipalo K., Aalto P., Vana M., Mirme A., Mirme S., Horrak U., Plass-Dülmer C., Stange G., Kiss G., Hoffer A., Törö N., Moerman M., Henzing B., de Leeuw G., Brinkenberg M., Kouvarakis G.N., Bougiatioti A., Mihalopoulos N., O'Dowd C., Ceburnis D., Arneth A., Svenningsson B., Swietlicki E., Tarozzi L., Decesari S., Facchini M.C., Birmili W., Sonntag A., Wiedensohler A., Boulon J., Sellegri K., Laj P., Gysel M., Bukowiecki N., Weingartner E., Wehrle G., Laaksonen A., Hamed A., Joutsensaari J., Petäjä T., Kerminen V.-M. & Kulmala M. 2010. EUCAARI ion spectrometer measurements at 12 European sites — analysis of new particle formation events. *Atmospheric Chemistry and Physics* 10: 7907–7927.

Mirme S. & Mirme A. 2013. The mathematical principles and design of the NAIS — a spectrometer for the measurement of cluster ion and nanometer aerosol size distributions. *Atmospheric Measurement Techniques* 6: 1061–1071.

Mirme S., Mirme A., Minikin A., Petzold A., Horrak U., Kerminen V.-M. & Kulmala M. 2010. Atmospheric sub-3 nm particles at high altitudes. *Atmospheric Chemistry and Physics* 10: 437–451.

Rose C., Boulon J., Hervo M., Holmgren H., Asmi E., Ramonet M., Laj P. & Sellegri K. 2013. Long-term observations of cluster ion concentration, sources and sinks in clear sky conditions at the high-altitude site of the Puy de Dome, France. *Atmospheric Chemistry and Physics* 13: 11573–11594.

Rose C., Sellegri K., Velarde F., Moreno I., Ramonet M., Weinhold K., Krejci R., Ginot P., Andrade M., Wiedensohler A. & Laj P. 2015. Frequent nucleation events at the high altitude station of Chacaltaya (5240 m a.s.l.), Bolivia. *Atmospheric Environment* 102: 18–29.

Tammet H. 2006. Continuous scanning of the mobility and size distribution of charged clusters and nanometer particles in atmospheric air and the Balanced Scanning Mobility Analyzer BSMA. *Atmospheric Research* 82: 523–535.

Ude S. & de la Mora J.F. 2005. Molecular monodisperse mobility and mass standards from electrosprays of tetra-alkyl ammonium halides. *Journal of Aerosol Science* 36: 1224–1237.

Winkler P.M., Steiner G., Vrtala A., Vehkamäki H., Noppel M., Lehtinen K.E.J., Reischl G.P., Wagner P.E. & Kulmala M. 2008. Heterogeneous nucleation experiments bridging the scale from molecular ion clusters to nanoparticles. *Science* 319: 1374–1377.

Winklmayr W., Reischl G.P., Lindner A.O. & Berner A. 1991. A new electromobility spectrometer for the measurement of aerosol size distributions in the size range from 1 to 1000 nm. *Journal of Aerosol Science* 22: 289–296.

Zhao J., Smith J.N., Eisele F.L., Chen M., Kuang C. &

McMurry P.H. 2011. Observation of neutral sulfuric acid–amine containing clusters in laboratory and ambient measurements. *Atmospheric Chemistry and Physics* 11: 10823–10836.